

daf-2, an Insulin Receptor–Like Gene That Regulates Longevity and Diapause in *Caenorhabditis elegans*

Koutarou D. Kimura,* Heidi A. Tissenbaum,* Yanxia Liu, Gary Ruvkun†

A *C. elegans* neurosecretory signaling system regulates whether animals enter the reproductive life cycle or arrest development at the long-lived dauer diapause stage. *daf-2*, a key gene in the genetic pathway that mediates this endocrine signaling, encodes an insulin receptor family member. Decreases in DAF-2 signaling induce metabolic and developmental changes, as in mammalian metabolic control by the insulin receptor. Decreased DAF-2 signaling also causes an increase in life-span. Life-span regulation by insulin-like metabolic control is analogous to mammalian longevity enhancement induced by caloric restriction, suggesting a general link between metabolism, diapause, and longevity.

A reversible arrest of *C. elegans* development at the metabolically less active dauer stage is triggered by a dauer-inducing pheromone (1). This pheromone is detected by sensory neurons, which then signal by a complex pathway to target tissues, such as the germ line, pharynx, intestine, and ectoderm, that are remodeled and metabolically shifted (1). Genetic analysis of *daf* mutants, which arrest at the dauer stage or enter the reproductive life cycle independent of pheromone regulation, has revealed that parallel genetic pathways regulate distinct aspects of the dauer metamorphosis (2). The pathway that includes *daf-2* controls both reproductive development and normal senescence: *daf-2* mutant animals arrest development at the dauer larval stage and exhibit a marked increase in longevity (1–3).

Genetic mapping, using both visible genetic markers and restriction fragment length polymorphism (RFLP) markers, placed *daf-2* between *mgP34* and *mgP44* (Fig. 1). Yeast artificial chromosome (YAC) Y53G8 carries the genomic region that includes *mgP34* and *mgP44*, which flank *daf-2* (Fig. 1). Analysis of 570 random Y53G8 M13 subclone DNA sequences from the Genome Sequencing Center revealed that four sequences (00667, 00622, 00318, and 00706) were homologous to regions of the mammalian insulin receptor family. The detection of multiple *daf-2* mutations in the gene (see below), and the coincidence of the genetic location of this insulin receptor homolog with *daf-2* (Fig. 1) establish that this insulin receptor homolog corresponds to *daf-2*.

The *daf-2* gene structure and DNA sequence were determined with the use of polymerase chain reaction (PCR) primers derived from *daf-2* genomic subclone sequences to amplify *daf-2* genomic and cDNA regions (Fig. 1, GenBank accession number AF012437). The predicted DAF-2 protein is 35% identical to the human insulin receptor, 34% identical to the human insulin-like growth factor–I (IGF-I) receptor, and 33% identical to the human insulin receptor–related receptor (4). DAF-2 is the

only member of the insulin receptor family in the 90-Mb *C. elegans* genome sequence (~90% complete) or in the 10-Mb *C. elegans* expressed sequence tag database. Because it is equally distant from the human insulin, IGF-I, and insulin receptor–related receptors, DAF-2 is probably the homolog of the ancestor of these duplicated and diverged receptors, and thus may subserve any or all of their functions. Like these receptors, DAF-2 has a putative signal peptide, a cysteine-rich region in the putative ligand-binding domain, a probable proteolysis site, a transmembrane domain, and a tyrosine kinase domain (Fig. 1); in addition, DAF-2 has a COOH-terminal region that may serve a function similar to that of mammalian insulin receptor substrate–1 (IRS-1) (Fig. 2) (5).

In the ~500–amino acid ligand-binding domain, DAF-2 is 36% identical to the insulin receptor and 35% identical to the IGF-I receptor. Of 23 phylogenetically conserved cysteine residues in this domain, 21 are conserved in DAF-2 (Fig. 2). The DAF-2 Cys-rich region is 34% identical to the insulin receptor and 28% identical to the IGF-I receptor. Six *daf-2* mutations map in this domain (Fig. 2 and Table 1). The *mg43* and *sa187* mutations substitute conserved residues in the Cys-rich region (Fig. 2). Other substitutions at nonconserved residues cause less severe phenotypes (Table 1).

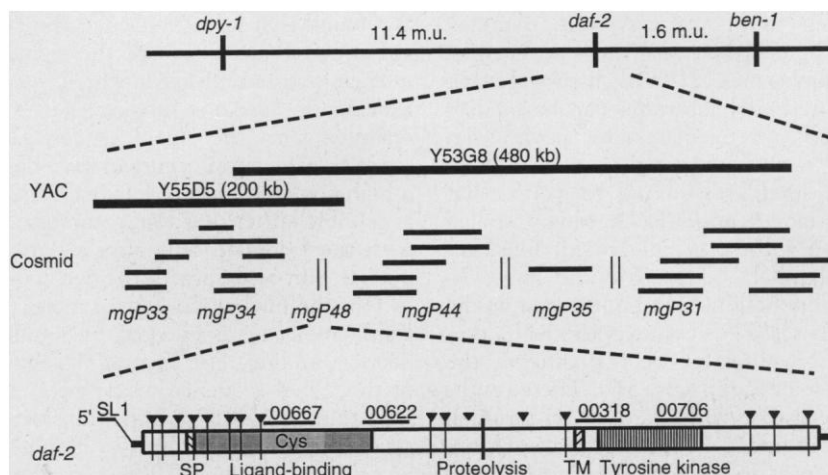


Fig. 1. Genetic and physical map of *daf-2*. *daf-2* maps between *mgP34* and *mgP44* in a region not covered by cosmid clones but covered by YAC Y53G8. Cosmids from the region detect RFLPs between *C. elegans* strains Bristol N2 and Bergerac RC301. Using 33 recombinants in the *dpy-1 daf-2* interval and 24 recombinants in the *daf-2 ben-1* interval, we were able to map *daf-2* 0.7 map units (m.u.) to the right of *mgP34* and 0.7 map units to the left of *mgP44*. Y53G8 YAC DNA hybridizes to multiple restriction fragments from cosmids bearing *mgP34* and *mgP44*. A probe from the insulin receptor homolog on Y53G8 detects the *mgP48* RFLP. *daf-2* could not be separated from this insulin receptor gene in 47 recombination events in a 13–map unit interval. The initial insulin receptor homolog shotgun sequences (00667, 00622, 00318, and 00706) are shown as thin bars above a box corresponding to *daf-2* cDNA. A probable full-length *daf-2* cDNA bears an SL1 transspliced leader (25), a 120-base 5' untranslated region (UTR), a 538-base open reading frame, and a 159-base 3' UTR. SP and TM denote putative signal peptide and transmembrane region, respectively. Intron positions (triangles) and lengths were detected by genomic and cDNA sequence and PCR amplification comparisons. The minimum *daf-2* gene size, based on this analysis, is 33 kb.

Department of Molecular Biology, Massachusetts General Hospital, and Department of Genetics, Harvard Medical School, Boston, MA 02114, USA.

*These authors contributed equally to this report.

†To whom correspondence should be addressed. E-mail: ruvkun@opal.mgh.harvard.edu

The 275-amino acid DAF-2 tyrosine kinase domain is 70% similar and 50% identical to the human insulin receptor kinase domain. Eight amino acid residues mediate target site specificity of the insulin receptor kinase (6); in DAF-2, six of these residues are invariant and two are replaced with similar amino acids (Fig. 2), which suggests that DAF-2 phosphorylates similar target tyrosine motifs to the insulin receptor kinase. Multiple DAF-2 tyrosine residues in

conserved sequence contexts and analogous positions are likely autophosphorylation targets (7) (Table 2). Three *daf-2* missense mutations substitute conserved amino acid residues in the kinase domain (Fig. 2 and Table 1). All three mutations cause moderate to strong dauer-constitutive phenotype, but none are as strong as the nonconditional alleles, for example, *mg43* (Table 1). Remarkably, a human diabetic insulin-resistant patient bears the same amino acid

substitution (Pro¹¹⁷⁸ → Leu) as *daf-2* (*e1391*) (Fig. 2) (8). This patient was reported to be heterozygous for this substitution. *daf-2(e1391)* is not dominant (9). It is possible that the patient was a compound heterozygote or carries mutations in other genes (for example, other complex type II diabetes loci) that enhance the dominance of Pro¹¹⁷⁸ → Leu (10).

Like the *Drosophila* insulin receptor homolog (11), DAF-2 has a long COOH-

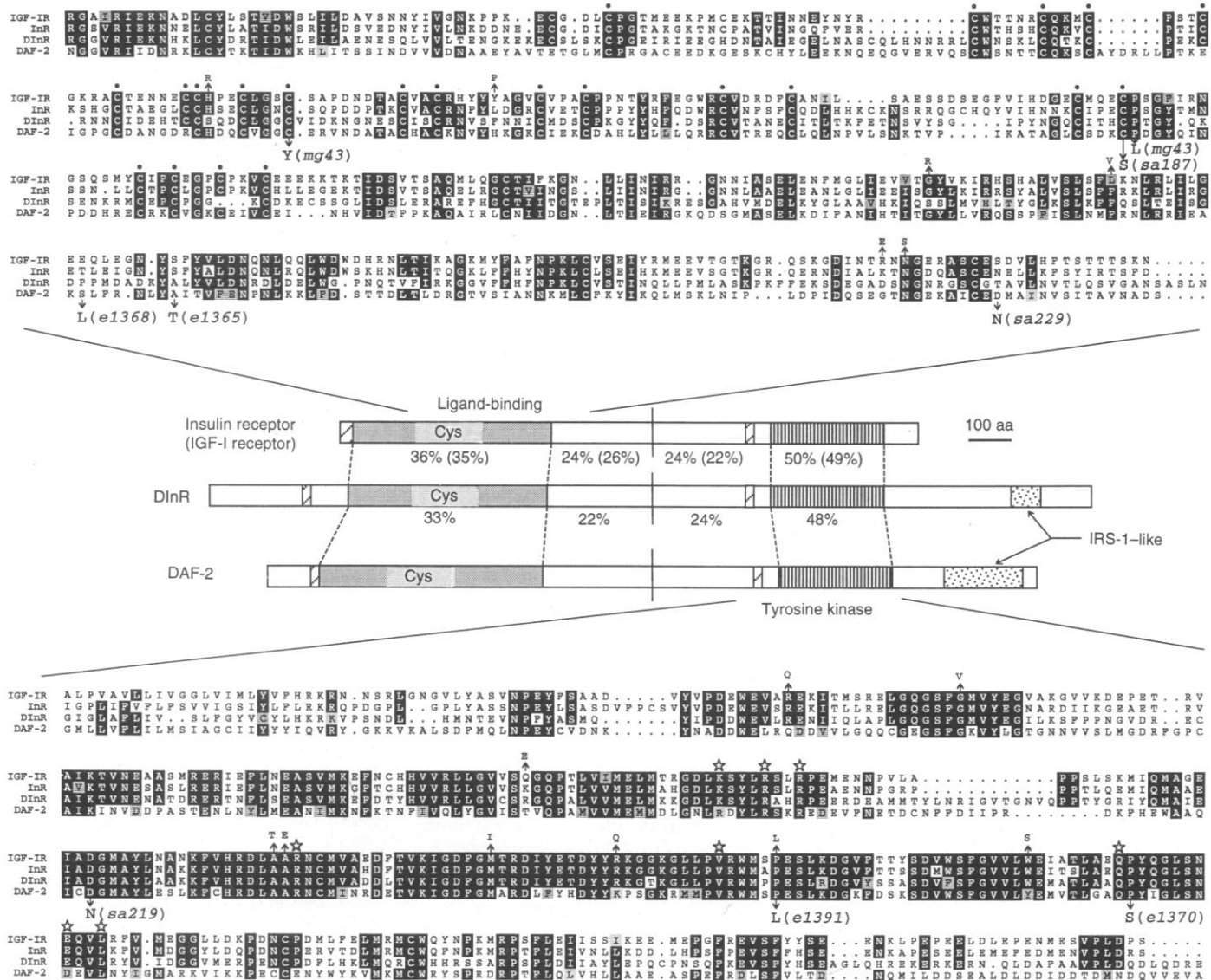


Fig. 2. Comparison of DAF-2 ligand-binding and kinase domains to insulin receptor family members. The amino acid comparison of DAF-2 to the human insulin receptor (InR) and IGF-I receptor (IGF-IR) and to the *Drosophila* insulin receptor homolog (DlnR) shown. The mutations found in human patients are indicated at the top of the rows, and *daf-2* allele substitutions are indicated below with allele names. Six *daf-2* mutations map in the ligand-binding domain: *sa187* (C469S, TGT to AGT), *e1368* (S573L, TCA to TTA), *e1365* (A580T, GCT to ACT), *sa229* (D648N, GAT to AAT), and two mutations in *mg43* (C401Y, TGT to TAT; P470L, CCC to CTC). Three *daf-2* mutations substitute conserved amino acid residues in the insulin receptor kinase domain: *sa219* (D1374N, GAT to

AAT), *e1391* (P1434L, CCC to CTC), and *e1370* (P1465S, CCA to TCA). Residues with black and shaded backgrounds indicate amino acid identity and similarity, respectively. The percentages under each domain represent the percentage identity between DAF-2 and each receptor. Conserved cysteine residues in the ligand-binding domain (top) are marked with dots. In the kinase domain, active-site residues that mediate insulin receptor kinase specificity are marked with stars. All of these residues are homologous in DAF-2. Abbreviations for the amino acid residues are as follows: A, Ala; C, Cys; D, Asp; E, Glu; F, Phe; G, Gly; H, His; I, Ile; K, Lys; L, Leu; M, Met; N, Asn; P, Pro; Q, Gln; R, Arg; S, Ser; T, Thr; V, Val; W, Trp; and Y, Tyr.

terminal extension that may function analogously to mammalian IRS-1, which is phosphorylated by the insulin receptor to recruit signaling proteins bearing Src homology 2 (SH2) domains (5). Many of the DAF-2 COOH-terminal extension tyrosines bear flanking sequence motifs (7) that suggest they are autophosphorylated (Table 2). On the basis of precedents from IRS-1 interactions with mammalian phosphatidylinositol (PI) 3-kinases (5), a Tyr-X-X-Met motif at DAF-2 Tyr¹⁶²⁶ is likely to mediate interaction with the AGE-1 PI 3-kinase, which acts in the same genetic pathway as *daf-2* to signal reproductive development and normal senescence (Fig. 3) (2, 3, 5, 12, 13). The insulin receptor also couples to other signaling pathways (5); analogous DAF-2 phosphotyrosine residues may mediate these interactions (Table 2) (13).

Insulin and its receptor families play key roles in vertebrate metabolic and growth

control (5). Upon stimulation of pancreatic insulin release by increasing blood glucose and autonomic inputs, insulin receptor engagement causes shifts in the activities of key metabolic enzymes, as well as changes in the transcription and translation of metabolic regulators in fat, liver, and muscle cells, all of which lead to assimilation of glucose into glycogen and fat and inhibition of glucose synthesis (5).

Diapause arrest in general and dauer arrest in particular are also associated with major metabolic changes (14), consistent with a model in which *daf-2* acts in a metabolic regulatory pathway related to insulin signaling. In wild-type animals, DAF-2 signaling allows nondauer reproductive growth, which is associated with the use of food (for growth in cell number and size) and with small stores of fat (Fig. 4). In *daf-2* mutant animals, metabolism is shifted to the production of fat (Fig. 4) and glyco-

gen (9) in intestinal and hypodermal cells. Even when a temperature-sensitive *daf-2* mutant allele is shifted to the nonpermissive temperature at the L4 or adult stage (after the critical period for *daf-2* control of dauer formation) (1), metabolism is shifted toward storage of fat (Fig. 4). Similar metabolic shifts are seen in wild-type pheromone-induced dauers, *age-1*, and *daf-7* mutants (Fig. 4) (9). In support of this metabolic shift, in dauer larvae, enzymes that regulate glycolysis are down-regulated while those that regulate glycogen and fat synthesis are up-regulated, and there is ultrastructural evidence for increased lipid and glycogen (14).

Even though DAF-2 and the mammalian insulin receptor both regulate metabolism, the metabolic defects associated with mutations in these receptors appear to be different. Complete loss of mammalian insulin receptor activity causes growth arrest at birth (leprechaunism in humans) and a metabolic shift to runaway lipolysis and ketoacidosis (5), rather than the fat accumulation we observe in *daf-2* mutants (Fig. 4). This distinction between insulin receptor and *daf-2* mutants may reflect distinct metabolic responses to this signaling, or a difference between complete loss and declines in insulin signaling. Because none of the *daf-2* mutations we have so far identified are clear null mutations, it is possible that *daf-2* dauer-constitutive alleles are more analogous to non-null human insulin receptor mutations (5). In fact, the 14-year-old patient with the same insulin receptor mutation as *daf-2*(*e1391*) was morbidly obese (8), suggesting that the metabolic effects of decreased insulin signaling may be similar to those of *daf-2* mutants.

The structural and functional homology of DAF-2 to the mammalian insulin receptor suggests that components of the insulin signaling pathway may act in metabolic and diapause control in *C. elegans*. There is precedent for invertebrate metabolic and growth control by insulin superfamily sig-

Fig. 3. A model of insulin-like signaling in the *C. elegans* dauer formation pathway. In the absence of dauer pheromone, an insulin-like ligand activates DAF-2, and a DAF-7 TGF- β -like signal activates the DAF-1 and DAF-4 receptors. Activated DAF-2 recruits AGE-1, which produces the second messenger PIP₃. This second messenger may regulate glucose transport (5), metabolic kinase cascades that include AKT and GSK-3 (16), and transcription and translation of metabolic genes (5). DAF-16 acts downstream of DAF-2 and AGE-1 in this pathway and is negatively regulated by them (2).

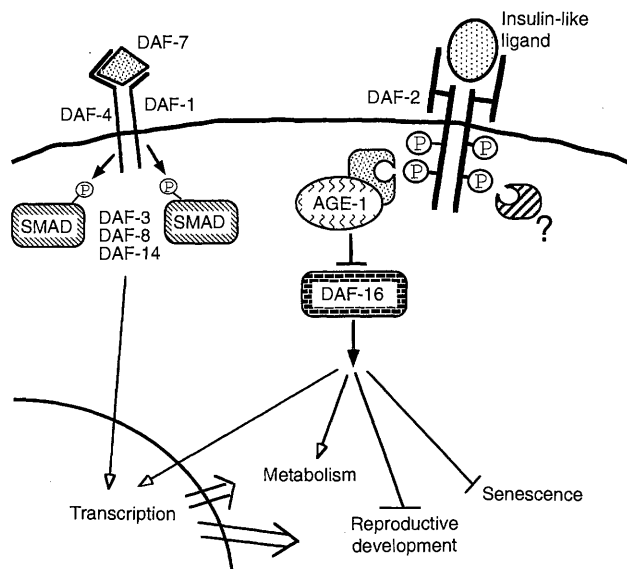


Table 1. Percentage dauer formation of *daf-2* alleles (*N*, number of animals). Eggs from animals grown at 15°C (day 0) were incubated at 15°, 20°, or 25°C. Numbers of wild-type animals and dauers were counted on day 3 (20° and 25°C) or day 5 (15°C). The dauers marked with asterisks recovered by day 4 (*sa229* at 25°C) or by day 8. *sa187* and *sa229* were also studied (27). Amino acid abbreviations are as in Fig. 2. ND, not determined.

Allele	Region	Mutation	Dauer formation			
			15°C % (N)	20°C % (N)	25°C % (N)	
N2		Wild type	0	0	0	
<i>mg43</i>	Ligand-binding	Cys-rich [C401Y, P470L	100.0 (215)	100.0 (245)	ND	
<i>sa187</i>			C469S	0.4 (461)	98.7 (224)	100 (910)
<i>e1368</i>			S573L	0.0 (328)	4.5* (418)	99.7* (698)
<i>e1365</i>	Kinase	A580T	0.0 (450)	0.0 (461)	99.4* (814)	
<i>sa229</i>			D648N	3.4* (234)	ND	22.1* (420)
<i>sa219</i>			D1374N	10.0* (460)	99.7* (396)	100 (514)
<i>e1391</i>	Kinase	P1434L	3.3 (332)	100 (323)	100 (322)	
<i>e1370</i>			P1465S	0.0 (520)	0.0 (188)	100 (635)

Table 2. Sequence motifs in the DAF-2 amino acid sequence. Amino acid abbreviations are as in Fig. 2. PTB, phosphotyrosine-binding domain.

Motif	Amino acids
Proteolysis site	RVRR(928-931)
PTB-binding	NPEY(1225-1228)
Three Tyr in the activation loop	DLFYHDYY(1412-1419)
SH2-binding (p85 subunit of PI 3-kinase)	DEEYALM(1623-1629)
SH2-binding (SHP-2 or PLC- γ)	DGDYIET(1797-1803)
SH2-binding (SEM-5)	EPKNYRNN(1804-1811)

naling (15). We hypothesize that an insulin-like signal is up-regulated during *C. elegans* reproductive development and stimulates DAF-2 receptor autophosphorylation and recruitment of the AGE-1 PI 3-kinase to produce the second messenger phosphatidylinositol-3,4,5-trisphosphate (PIP₃). AGE-1 is likely to be a major signaling output of DAF-2 because of the similarity of the *age-1* and *daf-2* mutant phenotypes and because of their similar placement in the epistasis pathway (2, 12) (Fig. 3). Precedent from insulin signaling suggests that PIP₃ activates membrane fusion of vesicles bearing sugar transporters, an AKT-GSK-3 kinase cascade (16) to regulate the activities of glycogen and fat synthetic and lytic enzymes, and the transcription and translation of metabolic genes such as those that encode PEPCCK and lipases (5).

Conversely, *C. elegans* *daf* genes may identify components of the mammalian insulin signaling pathway or converging pathways. The major target of DAF-2-AGE-1 signaling in *C. elegans* is DAF-16 (2). Mammalian homologs of DAF-16 may represent the output of insulin signaling. The dauer genetic pathway also suggests that DAF-7 transforming growth factor- β (TGF- β) neuroendocrine signals act in addition to DAF-2 insulin-like regulation of metabolism (Fig. 4) (17). Mammalian homologs of DAF-7 and its downstream signaling cascade (18) may represent signals that converge with insulin signals. Human ho-

mologs of the *daf* genes may be defective in diabetic pedigrees or inactivated in obesity-onset diabetes (19).

The DAF-2 receptor may act in the hypodermal and intestinal target tissues, where a change in metabolism is triggered by the dauer regulatory cascade (Fig. 4). It is also possible that DAF-2 regulates the metabolism and remodeling of tissues indirectly, for example, by controlling the production of other hormones (20). Expression and genetic mosaic analysis of *daf-2* is essential to distinguish these models.

In addition to these metabolic changes, the DAF-2 signaling cascade also controls the reproductive maturation of the germ line as well as morphogenetic aspects of the pharynx and hypodermis (1). This growth control by *daf-2* may be homologous to that mediated by the mammalian IGF-I receptor, which acts downstream of growth hormone (21). Like *daf-2* mutants, life-span is markedly increased in dwarf mice with defects in growth hormone signaling and, presumably, decreased IGF-I signaling (21).

Weak *daf-2* and *age-1* mutants that do not arrest at the dauer stage nevertheless live much longer than the wild type (3, 12). This connection between longevity and diapause control may not be unique to *C. elegans*. Diapause arrest is an essential feature of many vertebrate and invertebrate life cycles, especially in regions with seasonal temperature and humidity extremes (14). Animals in diapause slow

their metabolism and rates of aging and can survive for periods much longer than their reproductive life-span (14). Thus, partial induction of diapause by environmental conditions or genetic predispositions may underlie variations in life-span within and between species.

The increase in longevity associated with decreased DAF-2 signaling is analogous to mammalian longevity increases associated with caloric restriction (22). It is possible that caloric restriction causes a decline in insulin signaling to induce a partial diapause state, like that induced in weak *daf-2* and *age-1* mutants. The induction of diapause-like states, or changes in the mode and tempo of metabolism itself, may affect postreproductive longevity (22), as in *C. elegans*. This association of metabolic rate with longevity is also consistent with the correlation of free radical generation with aging (22).

Just as environmental extremes can select for variation in the genetic pathways that regulate *C. elegans* dauer formation, famines and droughts in human history may have selected for analogous variants in the human homologs of the *daf* genes. In fact, heterozygous mice carrying either the *db* or *ob* recessive diabetes genes survive fasting about 20% longer than do wild-type controls (23). The high frequency of type II diabetes in many human populations (19) may be the legacy of such selections.

REFERENCES AND NOTES

1. D. L. Riddle, in *Caenorhabditis elegans*, D. Riddle, T. Blumenthal, B. Meyer, J. Priess, Ed. (Cold Spring Harbor Laboratory Press, Cold Spring Harbor, NY, 1997), pp. 739-768; C. Kenyon, *ibid.*, pp. 791-813.
2. J. J. Vowels and J. H. Thomas, *Genetics* **130**, 105 (1992); S. Gottlieb and G. Ruvkun, *ibid.* **137**, 107 (1994); J. H. Thomas, D. A. Birnby, J. J. Vowels, *ibid.* **134**, 1105 (1993).
3. P. L. Larsen, P. S. Albert, D. L. Riddle, *ibid.* **139**, 1567 (1995); C. Kenyon, J. Chang, E. Gensch, A. Rudner, R. Tabtiang, *Nature* **366**, 461 (1993); J. B. Dorman, B. Albiner, T. Shroyer, C. Kenyon, *Genetics* **141**, 1399 (1995).
4. Y. Ebina *et al.*, *Cell* **40**, 747 (1985); A. Ullrich *et al.*, *Nature* **313**, 756 (1985); A. Ullrich *et al.*, *EMBO J.* **5**, 2503 (1986); P. Shier and V. M. Watt, *J. Biol. Chem.* **264**, 14605 (1989).
5. C. R. Kahn and G. C. Weir, Eds., *Joslin's Diabetes Mellitus* (Williams & Wilkins, Baltimore, MD, 1994).
6. S. R. Hubbard, L. Wei, L. Ellis, W. A. Hendrickson, *Nature* **372**, 746 (1994).
7. Z. Songyang and L. C. Cantley, *Trends Biochem. Sci.* **20**, 470 (1995).
8. H. Kim *et al.*, *Diabetologia* **35**, 261 (1992).
9. H. A. Tissenbaum, Y. Liu, G. Ruvkun, data not shown.
10. J. C. Bruning *et al.*, *Cell* **88**, 561 (1997).
11. R. Fernandez, D. Tabarini, N. Azpiazu, M. Frasch, J. Schlessinger, *EMBO J.* **14**, 3373 (1995).
12. J. Z. Morris, H. A. Tissenbaum, G. Ruvkun, *Nature* **382**, 536 (1996).
13. Although no p85-like adapter subunit has yet been detected in the *C. elegans* database, the AGE-1 homology to mammalian p110 suggests the existence of a homologous or analogous adapter (5). In the DAF-2 COOH-terminal domain, two other tyrosine residues may be autophosphorylated and

Fig. 4. Metabolic control by *daf-2* and *daf-7*. (A) Low accumulation of fat in a wild-type L3 animal grown at 25°C stained with sudan black (26). (B) Much more extensive fat accumulation in *daf-2* (*e1370*) grown at the nonpermissive temperature of 25°C. These animals accumulate fat in both intestinal and hypodermal cells. *daf-2* (*e1370*) animals grown at 15°C, the permissive temperature, accumulate small amounts of fat, like the wild type (9). (C) Extensive fat accumulation in the intestine and hypodermis of *daf-7* (*e1372*) animals grown at 25°C. (D) Extensive fat accumulation in *daf-2* (*e1370*) animals grown at the permissive temperature until the L4 stage and then shifted to the nonpermissive temperature. This shows that *daf-2* regulates metabolism without entry into the dauer stage.



- bound to particular SH2-containing proteins: Tyr¹⁸⁰⁰ binding to a phospholipase C- γ (PLC- γ) or SHP-2 homologs, and Tyr¹⁸⁰⁸ to SEM-5 (Table 2) (24).
14. M. J. Tauber, C. A. Tauber, S. Masaki, *Seasonal Adaptation of Insects* (Oxford Univ. Press, New York, 1986); V. B. O'Riordan and A. M. Burnell, *Comp. Biochem. Physiol.* **92B**, 233 (1989); *ibid.* **95B**, 125 (1990); J. D. Popham and J. M. Webster, *Can. J. Zool.* **57**, 794 (1978); W. G. Wadsworth and D. L. Riddle, *Dev. Biol.* **132**, 167 (1989).
 15. E. Roovers *et al.*, *Gene* **162**, 181 (1995); C. Hetru, K. W. Li, P. Bulet, M. Lagueux, J. A. Hoffmann, *Eur. J. Biochem.* **201**, 495 (1991); A. Kawakami *et al.*, *Proc. Natl. Acad. Sci. U.S.A.* **86**, 6843 (1989); M. Arpagaus, *Roux's Arch. Dev. Biol.* **196**, 527 (1987).
 16. B. A. Hemmings, *Science* **275**, 628 (1997).
 17. P. Ren *et al.*, *ibid.* **274**, 1389 (1996); W. S. Schackwitz, T. Inoue, J. H. Thomas, *Neuron* **17**, 719 (1996).
 18. L. L. Georgi, P. S. Albert, D. L. Riddle, *Cell* **61**, 635 (1990); M. Estevez *et al.*, *Nature* **365**, 644 (1993); G. I. Patterson, A. R. Kowock, A. Wang, Y. Liu, G. Ruvkun, unpublished data.
 19. C. R. Kahn, D. Vicent, A. Doria, *Annu. Rev. Med.* **47**, 509 (1996).
 20. H. Nagasawa *et al.*, *Science* **226**, 1344 (1984); E. A. Jonas *et al.*, *Nature* **385**, 343 (1997).
 21. L. S. Mathews, G. Norstedt, R. D. Palmiter, *Proc. Natl. Acad. Sci. U.S.A.* **83**, 9343 (1986); H. M. Brown-Borg, K. E. Borg, C. J. Meliska, A. Bartke, *Nature* **384**, 33 (1996).
 22. C. Finch, *Longevity, Senescence and the Genome* (Univ. of Chicago Press, Chicago, 1990).
 23. D. L. Coleman, *Science* **203**, 663 (1979).
 24. Z. Songyang *et al.*, *Cell* **72**, 767 (1993).
 25. M. Krause, in *Caenorhabditis elegans: Modern Biological Analysis of an Organism*, vol. 48 of *Methods in Cell Biology*, H. F. Epstein and D. C. Shakes, Eds. (Academic Press, San Diego, CA, 1995), p. 483.
 26. Nonstarved animals were fixed in 1% paraformaldehyde in phosphate-buffered saline, frozen at -70°C and washed, and then incubated overnight in sudan black.
 27. E. A. Malone and J. H. Thomas, *Genetics* **136**, 879 (1994).
 28. We thank A. Coulson, S. Chissoe, B. Waterston, T. Barnes, E. Zachgo, E. Malone, T. Inoue, J. Thomas, E. Lambie, J. Avruch, J. Kaplan, the Massachusetts General Hospital sequencing facility, the *C. elegans* Genetics Center, and the Ruvkun and Kaplan labs for assistance. K.D.K. is supported by the Japanese Society for the Promotion of Science. This work was supported by NIH grant RO1AG14161.

8 April 1997; accepted 26 June 1997

Synergistic Predation, Density Dependence, and Population Regulation in Marine Fish

Mark A. Hixon and Mark H. Carr*

Understanding natural causes of density dependence is essential for identifying possible sources of population regulation. Field experiments on a model system of coral reef fishes showed that small juveniles of *Chromis cyanea* suffer heavy mortality that is spatially density-dependent only in the presence of two suites of predators: transient piscivores attacking from above, and reef-resident piscivores attacking from below. In the absence of either kind of predator, early mortality of *Chromis* is virtually density-independent. Because piscivores may have regulatory roles in this and similar marine systems, overfishing these predators may have ramifications for the remainder of the exploited community.

Marine fish populations are notoriously dynamic (1). This is because of strong year-to-year variation in the recruitment of juveniles generated largely during the pelagic larval stage, when developing larvae are subject to various mortality sources that appear to be mostly density-independent (2). Despite these fluctuations, for any population neither to go extinct nor to increase without limit, at least one demographic rate must be density-dependent at some time and place (3–6). Here, we focus on the per capita (proportional) natural mortality rate, which is density-dependent if it increases with population size. Understanding such sources of population regulation is particularly timely as marine fisheries worldwide reach a state of crisis due mostly to overexploitation (7).

Detecting natural mechanisms of density dependence in exploited marine fishes has proven difficult because of a necessary reliance on indirect approaches based on often imprecise catch data, typically with high variance (1, 4). Nonetheless, correlative analyses of demersal (bottom-oriented) species indi-

cate that juveniles that have recently settled to the bottom may undergo density-dependent mortality (8), which often disappears in larger juvenile and adult stages (1, 9). Such analyses have been supplemented by recent small-scale field experiments with reef fishes suggesting that density-dependent mortality may occur within several weeks after settlement to a reef (5). However, the sources of density dependence remain largely unknown, although it is often hypothesized that predators cause density-dependent mortality of early juveniles of commercially valuable species (8, 9). Here, we provide experimental corroboration of this hypothesis by demonstrating spatial density dependence (6) in a coral reef fish.

Coral reef species provide excellent model systems for exploring density dependence after settlement in demersal fishes because they can be directly observed and experimentally manipulated in situ. New settlers and predators of our study species are particularly well-suited study subjects because they are easily counted, captured, and manipulated (10). We conducted our experiments on the Great Bahama Bank near the Caribbean Marine Research Center at Lee Stocking Island, Bahamas (10). Here, as elsewhere in this region, the plank-

tivorous damselfish *Chromis cyanea* (Pomacentridae) and other species are attacked by two suites of predators, which themselves are often the targets of fisheries: resident piscivores, mostly grouper (family Serranidae), that inhabit the same reef as their prey, and transient piscivores, mostly jack (family Carangidae), that regularly swim between reefs (11). Typical of elsewhere in their range, *Chromis* at this site occur in distinct aggregations of tens of individuals, each group centered on a prominent coral head, although fish within each aggregation are only loosely social relative to other group-living damselfish (12). Each summer, these aggregations are replenished by groups of several to tens of settling larvae that appear near each new moon (13).

The ideal experimental design to test for density-dependent mortality and any role of predation (as well as competition and recruitment limitation) is to manipulate orthogonally the density of the prey species and the presence of predators, then compare the subsequent survivorship of the prey among different treatments for a sufficient time (3, 5, 14). In the past, this design had proven extremely difficult to implement in studies of marine fishes because movement of both predators and prey between closely neighboring replicate sites rapidly swamped manipulations of local abundance (15). We overcame this problem by standardizing the isolation of coral patch reefs, which involved literally translocating live reefs, coral head by coral head, to a large sand flat behind the fore-reef from 1991 to 1993 (16). This effort produced a matrix of 32 similar natural reefs isolated by 200 m from each other and at least 1 km from the nearest nonexperimental reef (17). The location of this matrix was an area that received relatively few settling larvae (18). This allowed us to control the density of newly settled *Chromis* without the confounding effects of heavy natural settlement (10). The isolation of the reefs also effectively inhibited resident (not transient) piscivores from any tendency to emigrate to

M. A. Hixon, Department of Zoology, Oregon State University, Corvallis, OR 97331-2914, USA.

M. H. Carr, Department of Biology, University of California, Santa Cruz, CA 95064, USA.

*Authorship sequence determined by a coin toss.